JOM 23904

Mononuclear bis-aminocarbyne complexes of tungsten with Tp′ ligands; theory of metal-centred carbyne-carbyne coupling *

Alexander C. Filippou, Peter Hofmann, Paul Kiprof, Helmut R. Schmidt and Carola Wagner

Anorganisch-chemisches Institut der Technischen Universität München, Lichtenbergstraße 4, W-8046 Garching (Germany)

(Received April 30, 1993)

Abstract

An efficient procedure for the synthesis of mononuclear bis-aminocarbyne complexes of tungsten is reported starting from $Tp'(CO)_2W{\equiv}CN(R)Et$ (**1a**: R = Me; **1b**: R = Et) (Tp′ = hydrido(3,5-dimethylpyrazol-1-yl)borate). In the first step oxidative decarbonylation of **1a** and **1b** with Br_2 occurs to afford the six-coordinate aminocarbyne complexes $Tp'(Br)_2W{\equiv}CN(R)Et$ (**2a**, **2b**) in high yield. Similarly, complexes **1a** and **1b** are converted by I_2 into the diiodo derivatives $Tp'(I)_2W{\equiv}CN(R)Et$ (**3a**, **3b**). Reductive dehalogenation of **3a** and **3b** by Na/Hg in the presence of EtNC gives the electron-rich mono-aminocarbyne complexes $Tp'(EtNC)_2W{\equiv}CN(R)Et$ (**4a**, **4b**), which are finally alkylated with $[Et_3O]BF_4$ at one isocyanide-nitrogen to yield the bis-aminocarbyne complexes $\{Tp'(EtNC)W[\overset{..}{=}CN(R)Et][\overset{..}{=}CNEt_2]\}BF_4$ (**5a**, **5b**). Extended-Hückel calculations on the hypothetical 18e bis-carbyne complex $[CpW(CO)(CH)_2]^+$ predict a spontaneous rearrangement to the energetically favoured 16e acetylene complex $[CpW(CO)(HC{\equiv}CH)]^+$ and show, in full agreement with the experimental work, that introduction of amino-substituents on both carbyne-carbons stabilizes the bis-carbyne form relative to the alkyne isomer. The solid-state structure of **2b** was determined by a single-crystal X-ray diffraction study revealing a distorted octahedral complex with a short $W{-}C_{carbyne}$ bond. The short $C_{carbyne}{-}N$ bond and the planar amino-nitrogen indicate a high degree of π-bonding between the carbyne-carbon and the amino-nitrogen.

1. Introduction

The metal-centred coupling of two methylidyne ligands to form an acetylene ligand was first analyzed theoretically by R. Hoffmann *et al.* [1a,b]. These studies were performed for the "naked metal" case $M(CH)_2 \rightarrow M(C_2H_2)$ and have shown that the coupling reaction is symmetry-allowed for a d^2 to d^4 metal centre if the carbyne moiety is considered as a neutral 3e-donor ligand with a doubly occupied orbital of σ-symmetry and a pair of orthogonal acceptor orbitals of π-symmetry containing one electron [2*]. The "naked metal" case has also yielded some qualitative conclusions as to the effects of varying the metal and ligand properties in $L_nM(CR)_2$ systems [1a,b]. These have not been obtained, however, for specific and more realistic cases. In earlier work we had noticed in the metal-centred carbene–carbene coupling reaction and its reverse, the splitting of a coordinated olefin, that the "naked metal" model does not necessarily allow one to draw clearcut conclusions as to the energetic preference of substituted bis-carbene *vs.* olefin complexes [3]. Therefore, carbyne–carbyne coupling still poses some interesting theoretical questions.

Experimental work supports the theoretical predictions of Hoffmann for the metal-centred carbyne–carbyne coupling. Thus, reaction of the acyl-carbyne complex $Li[(Br)(CO)_2(L)\{\eta^1\text{-}C(O)Me\}W{\equiv}CR]$ with $C_2O_2Br_2$ and PPh_3 gives the alkyne coupling product $(Br)_2(CO)(PPh_3)(L)W(RC{\equiv}CMe)$ directly and not the d^4 tungsten bis-carbyne complex $(Br)_2(CO)(L)W(CR)(CMe)$ (L = CO, PPh_3; R = aryl) [4]. In comparison, stable d^4 molybdenum and tungsten bis-aminocarbyne complexes of the type *trans*-$\{(dppe)_2M[\overset{..}{=}CN(H)Me]_2\}(BF_4)_2$ (M = Mo, W) have been generated by double protonation of the electron-rich isocyanide complexes *trans*-$M(dppe)_2(CNMe)_2$ with HBF_4, indicating that the presence of a π-donor substituent at the carbyne-carbon stabilizes the bis-carbyne complex relative to the alkyne coupling product [5].

Correspondence to: Dr. A.C. Filippou.

* Herrn Professor Dr. Dr. h.c. mult. Ernst Otto Fischer in aufrichtiger Verbundenheit zum 75. Geburtstag gewidmet.

* Reference number with asterisk indicates a note in the list of references

0022-328X/93/$6.00

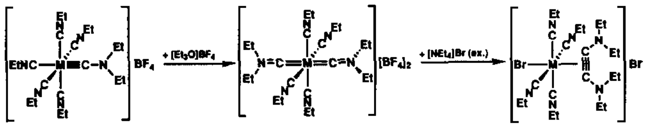

(1)

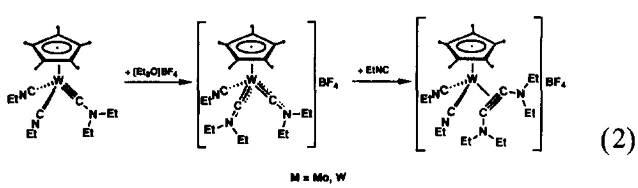

(2)

M = Mo, W

We have recently shown that a nucleophile-induced coupling of two carbyne ligands to give a coordinated alkyne (eqns. (1) and (2)) [6] is the carbon–carbon bond forming step in the acid-induced carbyne-isocyanide coupling reaction of Group VI transition metal complexes to give coordinated ynamines (eqn. (3)) [7] and the reductive isocyanide–isocyanide coupling reaction of $[M(CNR)_6X]^+$ complexes to give the ynediamine compounds $\{X(RNC)_4M[R(H)NC{\equiv}CN(H)R]\}^+$ (M = Mo^{II}, W^{II}; X = halogen; R = alkyl) [8].

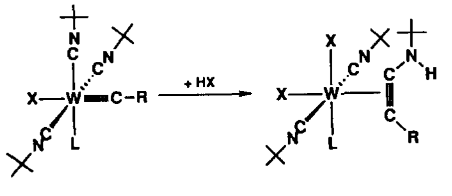

(3)

X = Br, I; R = Ph, NEt_2; L = CO, ${}^tBuNC$

In extension of this work, dealing with the interaction of two-faced π-ligands at a single metal center, we report here the high-yield synthesis of d^4 tungsten bis-aminocarbyne complexes starting from $Tp'(CO)_2W{\equiv}CN(R)Et$ (**1a**: R = Me; **1b**: R = Et) and Extended Hückel MO calculations on the hypothetical d^4 tungsten bis-carbyne complexes $[CpW(CO)(CH)_2]^+$ and $[CpW(CO)(CNH_2)_2]^+$, showing the effect of the π-donor substituent NH_2 at the carbyne-carbons on the relative stability of the 18e bis-carbyne complexes and their 16e alkyne coupling products $[CpW(CO)(HC{\equiv}CH)]^+$ and $[CpW(CO)(H_2NC{\equiv}CNH_2)]^+$, respectively.

The half-sandwich systems $[CpW(CO)(CR)_2]^+$ and $[CpW(CO)(RC{\equiv}CR)]^+$ were chosen as models because the metal fragment $[CpW(CO)]^+$ is related to the $[Tp'W(EtNC)]^+$ unit in this work and also ties in with our earlier work on analogous Cp* substituted compounds, summarized in eqn. (2).

2. Results and discussion

We have recently reported that half-sandwich bis-aminocarbyne complexes of the type $\{Cp^*(R'NC)W[{\equiv}CN(R')Et][{\equiv}CNEt_2]\}BF_4$ ($Cp^* = C_5Me_5$; R' = Et, ${}^tBu$) can be prepared in high yield starting from the dicarbonyl complex $Cp^*(CO)_2W{\equiv}CNEt_2$ [6a]. The synthetic procedure involves a stepwise transformation of the starting material to the electron-rich mono-aminocarbyne complexes $Cp^*(R'NC)_2W{\equiv}CNEt_2$, followed by the chemoselective alkylation of the latter at one isocyanide-nitrogen with $[Et_3O]BF_4$ [6a]. Application of the same methodology to the preparation of analogous Tp' complexes looked promising, since the desired starting materials, $Tp'(CO)_2W{\equiv}CN(R)Et$ (**1a**: R = Me; **1b**: R = Et) can be conveniently obtained from $W(CO)_6$ by high yield reactions which can be scaled-up to 10 g, and are thermally stable and easy to handle [9].

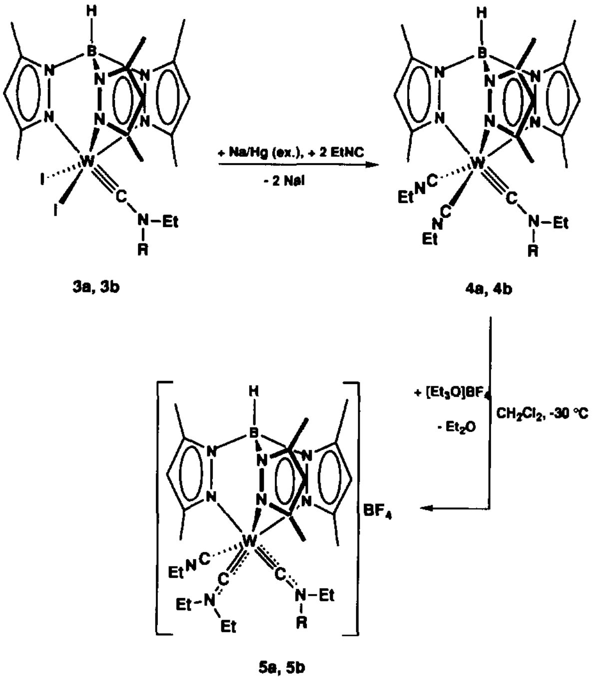

Scheme 1. Synthesis of Tp'-substituted bis-aminocarbyne tungsten complexes.

The three-step route followed for the synthesis of Tp' substituted bis-aminocarbyne complexes is depicted in eqn. (4) and Scheme 1. It begins with the oxidative decarbonylation of the dicarbonyl complexes **1a** and **1b** with X_2 (X = Br, I) to give the mono-aminocarbyne complexes $Tp'(X)_2W{\equiv}CN(R)Et$ (**2a**–**3b**) (eqn. (4)), followed by their reductive dehalogenation with Na/Hg in the presence of EtNC to afford the electron-rich mono-aminocarbyne complexes $Tp'(EtNC)_2W{\equiv}CN(R)Et$ (**4a**, **4b**) (Scheme 1). In the last step chemoselective ethylation of **4a** and **4b** at one isocyanide-nitrogen is achieved with $[Et_3O]BF_4$ to yield the desired bis-aminocarbyne complexes $\{Tp'(EtNC)W[{\equiv}CN(R)Et][{\equiv}CNEt_2]\}BF_4$ (**5a**, **5b**) (Scheme 1).

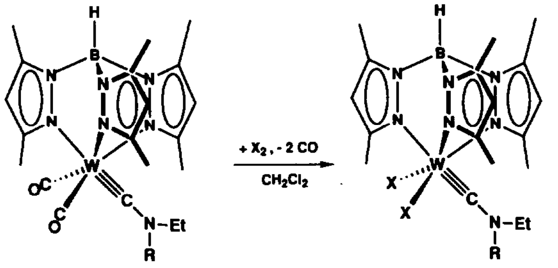

1a, 1b

2a–3b

(4)

	1a	1b	2a	2b	3a	3b
R	Me	Et	Me	Et	Me	Et
X	-	-	Br	Br	I	I

Oxidation of **1a** and **1b** with bromine was carried out in a 1/1 molar ratio in CH_2Cl_2 at room temperature and accompanied by evolution of gas (CO) and a fast colour change from yellow to blue. Evidence for the clean conversion of **1a** and **1b** to the octahedral dibromo complexes $Tp'(Br)_2W{\equiv}CN(R)Et$ (**2a**: R = Me; **2b**: R = Et) was given by the IR spectra of the reaction solutions, which revealed that the two strong ν(CO) absorptions of the starting materials **1a** and **1b** at 1936 and 1833 cm^{-1} had disappeared at the end of the reaction and their characteristic $\nu(C_{carbyne} \doteq N)$ absorptions at 1537 (**1a**) and 1528 cm^{-1} (**1b**) had been replaced by those of the products **2a** and **2b** at 1544 and 1532 cm^{-1}, respectively. Similarly, oxidation of **1a** and **1b** with a slight excess of iodine after prolonged refluxing in CH_2Cl_2 resulted in the clean formation of the six-coordinate, formally 16e complexes $Tp'(I)_2W{\equiv}CN(R)Et$ (**3a**: R = Me; **3b**: R = Et) (eqn. (4)). In comparison, oxidative decarbonylations of the Cp-analogues $(\eta^5\text{-}C_5R_5)(CO)_2M{\equiv}CNEt_2$ with one equivalent of $PhICl_2$, Br_2 or I_2 have been previously shown to afford the seven-coordinate, 18e aminocarbyne complexes $(\eta^5\text{-}C_5R_5)(X)_2(CO)M{\equiv}CNEt_2$ (R = H, Me; X = Cl, Br, I; M = Mo, W) (here the C_5R_5 ligand is considered to occupy three facial coordination sites) [10]. This difference in reactivity can be ascribed to the greater steric bulk of the Tp′ relative to the Cp and Cp* ligand destabilizing seven-coordinate species such as $Tp'(X)_2(CO)W{\equiv}CN(R)Et$ [9,11].

Complexes **2a**–**3b** were isolated, after purification by column chromatography on silica, as blue (**2a**, **2b**) and olive-green (**3a**, **3b**) solids in 77–86% yield. They are soluble in CH_2Cl_2 and THF, moderate soluble in Et_2O, but insoluble in n-pentane and show a remarkable thermal stability in crystalline form, decomposing in the temperature range 230–243°C.

Reductive dehalogenation of the diiodo complexes **3a** and **3b** was carried out in THF at room temperature using Na/Hg in the presence of EtNC and was accompanied by a fast colour change from green to orange and precipitation of NaI. Again IR monitoring of these reactions revealed a clean conversion of the starting materials to the electron-rich mono-aminocarbyne complexes $Tp'(EtNC)_2W{\equiv}CN(R)Et$ (**4a**: R = Me; **4b**: R = Et), which were isolated as yellow, microcrystalline solids in 72% and 61% yield, respectively (Scheme 1). Water and oxygen should be rigorously excluded in these syntheses. Otherwise formation of green by-products was observed, which were difficult to separate from **4a** and **4b**, causing a considerable decrease in the yield (purification of **4a** and **4b** by column chromatography on silica and neutral alumina was prevented by the fast decomposition of **4a** and **4b** on these supports).

Complexes **4a** and **4b** are soluble in all common organic solvents, decomposing at room temperature in $CHCl_3$ and CH_2Cl_2 due to oxidative degradation by the solvent. They are very oxygen- and water-sensitive, rapidly turning green in air. These properties indicate the presence of an electron-rich metal centre in **4a** and **4b**. Further experimental evidence for this is provided by the IR spectra of **4a** and **4b** revealing low-frequency $\nu(C{\equiv}NEt)$ absorptions, the ^{13}C NMR spectra showing unusually low-field chemical shifts of the metal-bonded isocyanide-carbons (see Spectroscopic investigations) and the fast reactions of these compounds with electrophiles. Thus, when complexes **4a** and **4b** were treated with one equivalent of $[Et_3O]BF_4$ in CH_2Cl_2 at −30°C, a fast reaction occurred to give selectively the bis-aminocarbyne complexes $\{Tp'(EtNC)W[\doteq CN(R)Et][\doteq CNEt_2]\}BF_4$ (**5a**: R = Me; **5b**: R = Et) (Scheme 1). No evidence of electrophilic addition at the metal centre was obtained in these reactions (IR monitoring), which represent another example of the activation of isocyanides for electrophilic attack at the nitrogen atom upon coordination to an electron-rich metal centre [5,6a,8d–f,9,11c].

Complexes **5a** and **5b** were isolated as yellow solids in 85% and 91% yield, respectively. They are soluble in CH_2Cl_2, but insoluble in Et_2O and n-pentane and decompose slowly in solution at room temperature. The stability of the bis-aminocarbyne complexes **5a** and **5b** results from the strong interaction of the p-type lone pair at the amino-nitrogen with one of the two vacant p orbitals at the carbyne-carbon. Experimental evidence for this π-interaction is provided by the IR-spectra of **5a** and **5b** revealing two characteristic low-frequency $\nu(C_{carbyne} \doteq N)$ absorptions at 1606 and 1526 cm^{-1} (**5a**) and 1602 and 1519 cm^{-1} (**5b**) (see Spectroscopic investigations). The role of this π-interaction in the electronic stabilization of the d^4 tungsten bis-aminocarbyne complexes **5a** and **5b** becomes evident, if one compares the results of Extended Hückel MO calculations on the hypothetical d^4 tungsten bis-carbyne complexes $[CpW(CO)(CH)_2]^+$ and $[Cp(CO)W(CNH_2)_2]^+$ (the carbyne fragment is again considered in all bis-carbyne complexes as a neutral 3e-donor ligand giving the tungsten centre a formal d^4 electron configuration) [2]. Figure 1 shows the interaction diagram between the d^4 metal fragment $[CpW(CO)]^+$ and the bis-carbyne fragment $(CH)_2$.

The valence orbitals of a "bent" CpML fragment have been discussed in detail elsewhere and need not be reiterated here [12]. For the chosen electron population of the $[CpW(CO)]^+$ fragment (d^4), the 2a′, 2a″ and 3a′ orbitals are empty and the bis-methylidyne unit on the right side of Fig. 1 carries 6 electrons in its six frontier MO's. These MO's are easily identified as the appropriate linear combination of the orbitals of a single CH group (C_s-symmetry labels were used for the $(CH)_2$ moiety as for the composite system $[CpW(CO)(CH)_2]^+$ and for the $[CpW(CO)]^+$ fragment). The lone pair MO's 1a′ and 1a″ of the $(CH)_2$ moiety interact strongly with the two empty metal MO's 2a″ and 3a′. The resulting 1a′ and 1a″ orbitals of the bis-methylidyne complex represent the two metal–methylidyne σ bonds, whereas the 2a′, 3a′ and 2a″ orbitals are the equivalent of three metal–methylidyne π bonds, showing that the metal centre is not able to form two independent metal–carbon triple bonds in this hypothetical molecule, as expected from simple electron counting. The out-of-phase combination 3a″ of the two in-plane methylidyne p-orbitals has the wrong pseudosymmetry to mix with any s, p or d metal orbital and, as a pure ligand-orbital, represents the LUMO (3a″) of the bis-methylidyne complex cation.

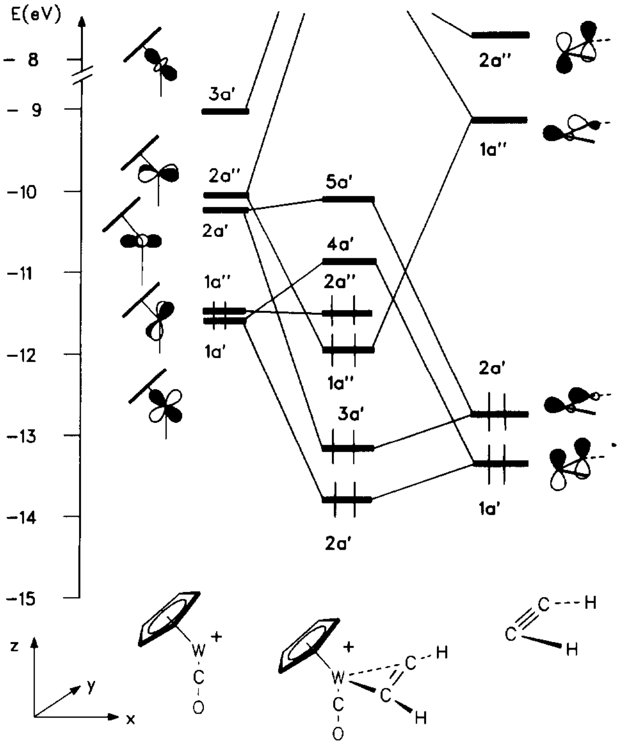

Fig. 2. Interaction diagram for $CpW(CO)(C_2H_2)^+$ between CpW $(CO)^+$ and a bent (C_2H_2) fragment.

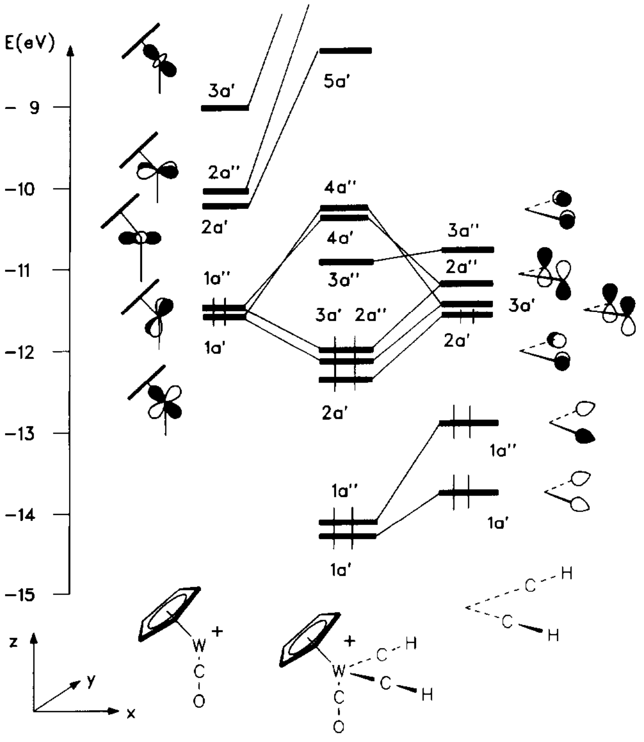

Fig. 1. Interaction diagram for $CpW(CO)(CH)_2{}^+$ between CpW$(CO)^+$ and a $(CH)_2$ fragment.

Figure 2 shows the analogous interaction diagram between the d^4 metal fragment $[CpW(CO)]^+$ and a neutral acetylene ligand. The 3a′ MO of the 16e-acetylene complex represents the metal–alkyne σ bond and the 2a′ orbital the alkyne to metal π-donation (the 1a′ MO, which corresponds to the C–C σ bond of the acetylene ligand, appears at a much lower energy and is not shown in Fig. 2). HOMO and LUMO of the complex (2a″ and 4a′) are nearly pure metal orbitals, whereas the out of plane π^*-orbital of the acetylene (2a″) is destabilized through interaction with the metal 1a″ orbital (mainly d_{yz}), leading to some out-of-plane back bonding from the tungsten centre to the acetylene ligand.

Figure 2 displays the typical picture of a 16e complex with a small HOMO–LUMO gap (2a″/4a′), which is related to the 18e system of Fig. 1 by a simple least motion process of reducing the C–W–C angle β in eqn. (5) and of simultaneously diminishing the W–C–H angle α on both metal carbyne sub-units.

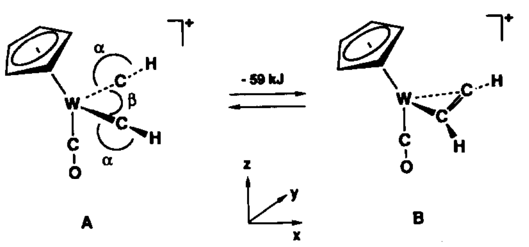

(5)

18e bis-methylidyne complex

16e acetylene complex

As the methylidyne ligands approach each other along this least motion pathway, orbitals which are symmetric to this motion within the *xy* plane, such as the 1a′ and 2a′ orbitals of the bis-methylidyne complex, are stabilized, whereas orbitals, which are antisymmetric to the *xz* plane, such as the 1a″ and 2a″ orbitals, are destabilized (Fig. 3). The 1a″, 2a′ and 3a′ orbitals of the bis-methylidyne complex are transformed into the acetylene–metal σ and π bonds, respectively, whereas the 2a″ orbital of the bis-methylidyne complex correlates to the out-of-plane metal–acetylene dπ–pπ back bond. Finally, the 1a′ MO of the bis-methylidyne complex becomes the acetylene C–C σ-orbital, whereas the 3a″ orbital correlates to the σ^* acetylene bond and rises sharply in energy.

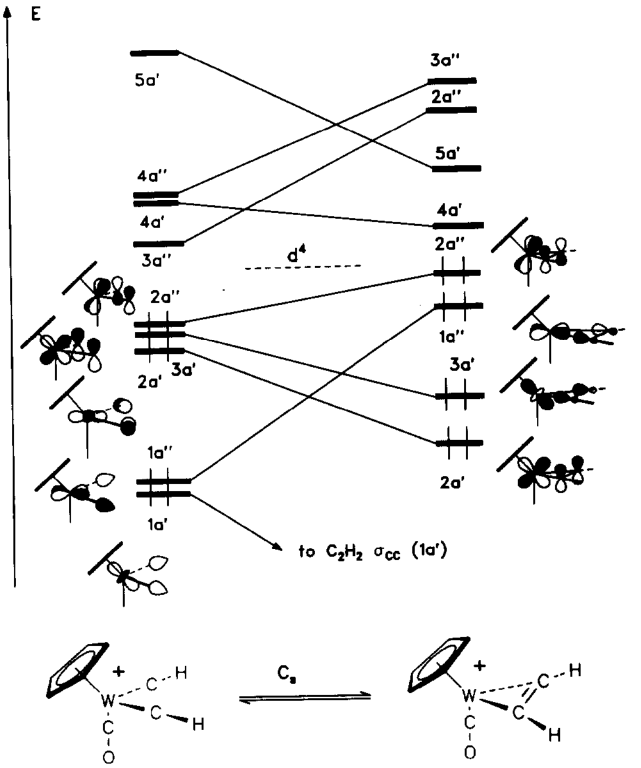

Fig. 3. MO correlation diagram for the least motion (C_s) CH/CH coupling of $CpW(CO)(CH)_2{}^+$ to $CpW(CO)(C_2H_2)^+$.

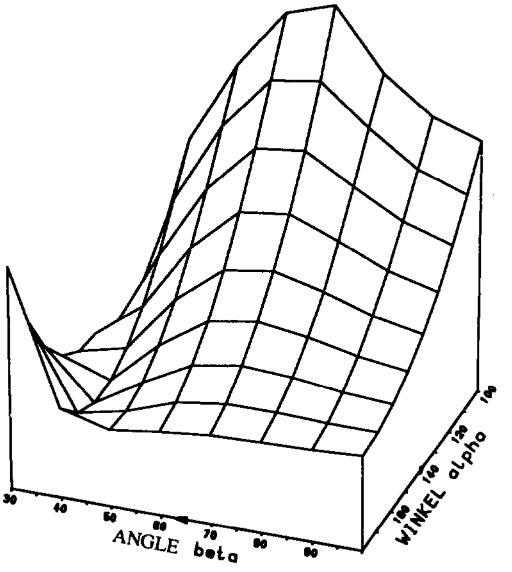

Fig. 4. $E_{\alpha,\beta}$ energy surface for the CH/CH coupling process in $[CpW(CO)(CH)_2]^+$.

Note that there are various avoided crossings, which are not displayed in detail in Fig. 3, *e.g.* the 1a′ orbital on the bis-methylidyne complex side wants to correlate to the 3a′ orbital of the coupling product, the 2a′ orbital of the bis-methylidyne complex is the equivalent of the acetylene C–C σ-orbital, whereas the 3a′ orbital on the left side is related to the 2a′ wavefunction on the right side of Fig. 3.

No crossing between filled and unfilled orbitals occurs along the least motion coupling pathway. Therefore, the coupling reaction is symmetry-allowed for a d^4 metal centre, as expected. Figure 3 does not allow an immediate conclusion as to the relative energy of the two interconverting systems or their interconversion barrier. However, if one computes a two dimensional energy surface for the CH/CH coupling process along the simplest least motion pathway, varying the two angular parameters α and β of eqn. (5), the bis-methylidyne complex **A** does not represent a minimum on the energy surface of the coupling reaction. The only minimum is found at $\alpha = 160°$ and $\beta = 40°$, which corresponds to an acetylene intermediate **B** with a C–C bond of 140 pm (Fig. 4).

As a consequence, no activation barrier exists for the transformation of the 18e bis-methylidyne complex **A** to the 16e acetylene intermediate **B**, which is more stable than **A** by 59 kJ (eqn. (5)). **B** is even further stabilized upon relaxation of its molecular geometry by alkyne rotation towards **B′** and by concomitant pyramidalization at the metal centre (eqn. (6)). However, according to our model calculations these geometry relaxation processes do not set in before the two CH ligands have formed the coordinated acetylene [13*]. We have not performed a full geometric search for the minimum structure of the 16e coupling product **B**, because the relevant part of our analysis focusses on the coupling step.

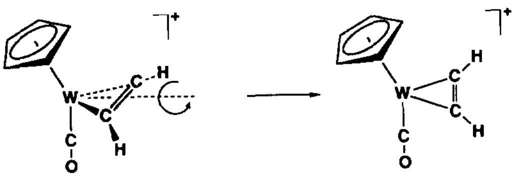
(6)

B **B'**

The 16e acetylene coupling product will obviously gain additional stability upon coordination of another 2e-donor ligand. However, it should be pointed out that interference of a nucleophile is not necessary to induce the coupling of the two methylidyne ligands, which is predicted to be a spontaneous, energetically favourable process for a d^4 metal electron count. The nucleophile simply acts as a trapping agent for the resulting 16e acetylene complex. All these results imply that d^4 bis-carbyne complexes, which do not bear π-donor substituents at the carbyne-carbons, are not intermediates in reactions where their formation might be inferred from the isolation of alkyne coupling products [4].

Let us now consider the analogous coupling reaction of two aminocarbynes to an ynediamine ligand at the same d^4 tungsten centre. Three possible conformers **C**–**E** may be envisaged for the d^4 bis-aminocarbyne complex $[CpW(CO)(CNH_2)_2]^+$, with their NH_2 planes perpendicular (90°) to or in the WC_2N_2 plane (0°) (Fig. 5).

Extended Hückel MO calculations show that conformer **D**, in which one amino plane is perpendicular to and one within the coupling plane, is more stable by 4.1 kJ than the less favoured conformer **C**, in which both amino planes are upright, and more stable by 23 kJ than conformer **E**. The activation barrier for the interconversion of the bis-aminocarbyne conformers is therefore very low. These results are in full agreement with the NMR spectroscopic data of the bis-aminocarbyne complexes **5a** and **5b**, which reveal a low activation barrier to rotation of the amino groups around the $C_{carbyne}$–N bonds, resulting in a rapid equilibration of all possible bis-aminocarbyne conformers on the NMR time scale.

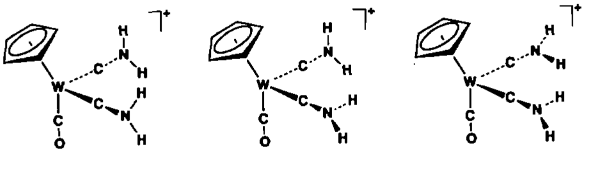
C (90°, 90°) D (90°, 0°) E (0°, 0°)

Fig. 5. Possible conformers for the hypothetical bis-aminocarbyne complex $[CpW(CO)(CNH_2)_2]^+$.

Similarly, several conformers may be envisaged for the 16e ynediamine least-motion coupling product. The calculations show that conformer **F** with a fully planar $C_2N_2H_4$ ligand (0°, 0°) is conformationally preferred, but less stable by *ca*. 65 kJ than its bis-aminocarbyne isomer **D** with 18 valence electrons (eqn. (7)).

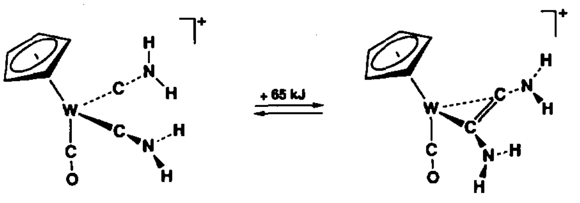

(7)

D (90°, 0°) F (0°, 0°)

18e bis-aminocarbyne complex

16e ynediamine complex

Again, an alkyne rotation after the coupling process would stabilize the conformer **F**, but still the resulting structure **G** is much less stable than either **C**, **D** or **E**.

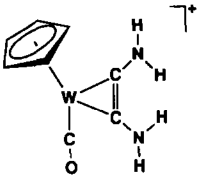
G

These results imply that a rotation of one amino group by 90° has to occur along the least motion coupling coordinate in order to convert the most stable bis-aminocarbyne conformer **D** to the most stable ynediamine conformer **F** (eqn. (7)). The isomerization of **D** to **F** is symmetry-allowed, as described above for the bis-methylidyne case. It is however energetically *unfavourable*, since the 18e bis-aminocarbyne complex **D** is more stable by 65 kJ than the 16e ynediamine coupling product **F** and represents the only minimum on the $E_{\alpha,\beta}$ coupling energy surface (Fig. 6) [14*]. Clearly, the NH_2 groups, being potent single-faced π-donor substituents, reverse the relative stability of the bis-carbyne and the alkyne complex isomers. This is a phenomenon which we have noted before in related studies on alkene formation (carbene–carbene coupling) and alkene-cleavage processes at a $Cr(CO)_4$

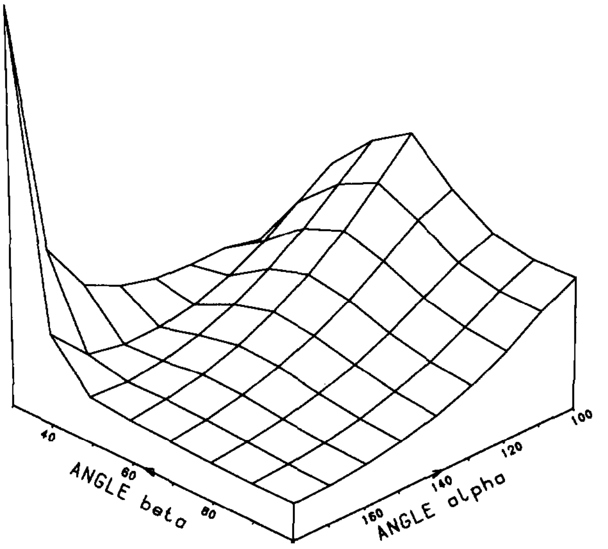

Fig. 6. $E_{\alpha,\beta}$ energy surface for the CNH_2/CNH_2 coupling process in $[CpW(CO)(CNH_2)_2]^+$.

fragment, showing that bis-aminocarbene complex isomers are more stable [15] and that tetrakis(amino)olefins are cleaved spontaneously at the metal centre [3].

Our theoretical predictions for the metal bis-carbyne complexes are supported by the present experimental work showing that the d^4 metal bis-aminocarbyne complexes $\{Tp'(EtNC)W[\overset{\cdots}{=}CN(R)Et][\overset{\cdots}{=}CNEt_2]\}BF_4$ (**5a**, **5b**) are stable, isolable compounds [6a].

As noted before, the addition of a nucleophile is expected to stabilize the 16e-ynediamine product **F**, changing the overall thermodynamics of the aminocarbyne-aminocarbyne coupling reaction of **D** (eqn. (7)). Indeed, reaction of the d^4 tungsten bis-aminocarbyne complex $[Cp^*(EtNC)W(\overset{\cdots}{=}CNEt_2)_2]BF_4$ with EtNC has been previously reported to give the bis(diethylamino)acetylene complex $[Cp^*(EtNC)_2W(Et_2NC{\equiv}CNEt_2)]BF_4$ [6a]. A question of obvious interest is how the bis(diethylamino)acetylene ligand is formed in this reaction, *i.e.* whether the nucleophile induces the carbyne–carbyne coupling reaction or simply adds to the metal centre after the alkyne C–C bond has been formed. Studies aimed at experimentally answering this question, as well as related theoretical work, are presently in progress.

3. Spectroscopic investigations

3.1. IR spectra

The mono-aminocarbyne complexes **2a**–**4b** are distinguished by one IR-absorption in the range 1544–1496 cm^{-1}, which is assigned to the $\nu(C_{carbyne} \overset{\cdots}{=} N)$ vibration (Table 1). The fairly high frequency of this absorption reveals a strong delocalization of the nitrogen lone pair electrons into one of the two vacant p-orbitals at the carbyne-carbon [5b,6b,9]. A comparison of the aminocarbyne complexes **2a**–**3b** with **4a** and **4b** reveals that the $\nu(C_{carbyne} \overset{\cdots}{=} N)$ absorption is shifted to lower wavenumbers as the electron density at the metal centre is increased (stronger metal–carbyne back bonding) [10b,10c,16]. Also consistent with this trend is the observation that the $\nu(C_{carbyne} \overset{\cdots}{=} N)$ absorptions of the diethylaminocarbyne complexes $Tp'(X)_2W{\equiv}CNEt_2$ (**2b**, **3b**) (Table 1) appear at considerably lower wavenumbers than those of the analogous carbonyl-containing compounds $Cp^*(X)_2(CO)W{\equiv}CNEt_2$ (X = Br, $\nu(C \overset{\cdots}{=} N)$ in CH_2Cl_2: 1603 cm^{-1}; X = I, $\nu(C \overset{\cdots}{=} N)$ in CH_2Cl_2: 1605 cm^{-1}) [16c], and that the $\nu(C_{carbyne} \overset{\cdots}{=} N)$ absorptions of the Tp′ complexes **4b** and **5b** (Table 1) are observed at lower frequencies than those of the analogous Cp* derivatives $Cp^*(EtNC)_2W{\equiv}CNEt_2$ [$\nu(C \overset{\cdots}{=} N)$ in n-pentane: 1511 cm^{-1}] and $[Cp^*(EtNC)W(\overset{\cdots}{=}CNEt_2)_2]BF_4$ [$\nu(C \overset{\cdots}{=} N)$ in CH_2Cl_2: 1610, 1539 cm^{-1}] [6a].

In comparison, the bis-aminocarbyne complexes are distinguished by two $\nu(C_{carbyne} \overset{\cdots}{=} N)$ absorptions at 1606 and 1526 cm^{-1} (**5a**) and 1602 and 1519 cm^{-1} (**5b**) (Table 1). The high frequency of these absorptions reveals that in both carbyne ligands extensive π-donation by the nitrogen lone pair occurs into one of the two carbyne-carbon p-orbitals. Such an interaction is represented in valence bond terms by the resonance forms **a**, **b** and **c** (Fig. 7). A "bis-carbyne" resonance form "$\{M[{\equiv}CN(R)Et]({\equiv}CNEt_2)\}$" is not appropriate to

TABLE 1. $\nu(BH)$, $\nu(C{\equiv}NEt)$ and $\nu(C \overset{\cdots}{=} N)$ absorptions of **2a**–**5b** in cm^{-1}; solvents: CH_2Cl_2 (a), n-pentane (b)

Complex	$\nu(BH)$	$\nu(C{\equiv}NEt)$	$\nu(C \overset{\cdots}{=} N)_{ring}$	$\nu(C_{carbyne} \overset{\cdots}{=} N)$	solvent
$Tp'(Br)_2W{\equiv}CN(Me)Et$ (**2a**)	2555w	–	1544s	1544s	a
$Tp'(Br)_2W{\equiv}CNEt_2$ (**2b**)	2555w	–	1543s	1532s	a
$Tp'(I)_2W{\equiv}CN(Me)Et$ (**3a**)	2556w	–	1544s	1544s	a
$Tp'(I)_2W{\equiv}CNEt_2$ (**3b**)	2556w	–	1542s	1532s	a
$Tp'(EtNC)_2W{\equiv}CN(Me)Et$ (**4a**)	2543vw, sh, 2524w	1890w, 1807s	1546m	1504m	b
$Tp'(EtNC)_2W{\equiv}CNEt_2$ (**4b**)	2543vw, sh, 2523w	1888w, 1807s	1546m	1496m	b
$\{Tp'(EtNC)W[\overset{\cdots}{=}CN(Me)Et][\overset{\cdots}{=}CNEt_2]\}BF_4$ (**5a**)	2556w	2199m, sh, 2186m	1544s	1606m, 1526s	a
$[Tp'(EtNC)W(\overset{\cdots}{=}CNEt_2)_2]BF_4$ (**5b**)	2557w	2195m, sh, 2186m	1544s	1602m, 1519s	a

TABLE 2. ^{1}H NMR data of the complexes **2a**–**5b**; relative intensities and multiplicities in parentheses, coupling constants in Hz

Complex	CH_3CH_2NC	$N(CH_2CH_3)_2$; $N(CH_3)CH_2CH_3$	Tp′-C*Me*	$N(CH_3)CH_2CH_3$; NCH_3	$N(CH_2CH_3)_2$	CH_3CH_2NC	Tp′-C*H*	solvent; *T* (°C)
2a	–	1.39 (3, t) ^3J(HH) = 7.3	2.56 (3, s); 2.61 (6, s); 2.65 (6, s); 2.87 (3, s)	6.55 (2, q) ^3J(HH) = 7.3; 7.27 (3, s)	–	–	5.88 (1, s); 6.05 (2, s)	CD_2Cl_2; +20
2b	–	1.31 (6, t) ^3J(HH) = 7.3	2.58 (3, s); 2.66 (6, s); 2.69 (6, s); 2.92 (3, s)	–	6.83 (4, q) ^3J(HH) = 7.3	–	5.88 (1, s); 6.06 (2, s)	CD_2Cl_2; +20
3a	–	1.49 (3, t) ^3J(HH) = 7.3	2.72 (6, s); 2.77 (6, s) 2.78 (3, s); 3.38 (3, s)	7.70 (2, q) ^3J(HH) = 7.3; 8.29 (3, s)	–	–	5.98 (2, s); 6.04 (1, s)	CD_2Cl_2; +20
3b	–	1.39 (6, t) ^3J(HH) = 7.3	2.76 (6, s); 2.78 (3, s); 2.79 (6, s); 3.41 (3, s)	–	7.94 (4, q) ^3J(HH) = 7.3	–	5.98 (2, s); 6.04 (1, s)	CD_2Cl_2; +20
4a	1.07 (6, t) ^3J(HH) = 7.3	1.19 (3, t) ^3J(HH) = 7.3	2.19 (9, s); 2.76 (3, s); 2.84 (6, s)	2.92 (3, s); 3.23 (2, q) ^3J(HH) = 7.3	–	3.42 (2, dq) ^2J(HH) = 13.4 ^3J(HH) = 7.3; 3.48 (2, dq) ^2J(HH) = 13.4 ^3J(HH) = 7.3	5.66 (1, s); 5.72 (2, s)	C_6D_6; +20
4b	1.10 (6, t) ^3J(HH) = 7.3	1.21 (6, t) ^3J(HH) = 7.3	2.19 (9, s); 2.74 (3, s); 2.85 (6, s)	–	3.25 (4, q) ^3J(HH) = 7.3	3.45 (2, dq) ^2J(HH) = 13.4 ^3J(HH) = 7.3; 3.51 (2, dq) ^2J(HH) = 13.4 ^3J(HH) = 7.3	5.66 (1, s); 5.73 (2, s)	C_6D_6; +20
5a	1.42 (3, t) ^3J(HH) = 7.3	1.25 (3, t) ^3J(HH) = 7.3; 1.29 (6, t) ^3J(HH) = 7.3	2.33 (3, s); 2.35 (3, s); 2.38 (3, s); 2.40 (3, s); 2.42 (3, s)	3.20 (3, s); 3.39 (1, dq) ^2J(HH) = 13.7 ^3J(HH) = 7.3; 3.46 (1, dq) ^2J(HH) = 13.7 ^3J(HH) = 7.3	3.34 (2, dq) ^2J(HH) = 13.7 ^3J(HH) = 7.3; 3.55 (2, dq) ^2J(HH) = 13.7 ^3J(HH) = 7.3	3.83 (2, q) [a] ^3J(HH) = 7.3	5.92 (1, s); 5.93 (1, s); 5.94 (1, s)	CD_2Cl_2; −60
5b	1.42 (3, t) ^3J(HH) = 7.3	1.29 (12, t) ^3J(HH) = 7.3	2.35 (3, s); 2.37 (6, s); 2.42 (6, s); 2.45 (3, s)	–	3.42 (4, dq) ^2J(HH) = 13.7 ^3J(HH) = 7.3; 3.57 (4, dq) ^2J(HH) = 13.7 ^3J(HH) = 7.3	3.85 (2, q) ^3J(HH) = 7.3	5.93 (2, s); 5.95 (1, s)	CD_2Cl_2; −30

[a] These methylene protons are by accident homotopic.

TABLE 3. ^{13}C-NMR data of the complexes **2a–5b**; coupling constants in Hz

Complex	Tp′C*Me*;	N(Me)$CH_2\mathit{C}H_3$	N($CH_2\mathit{C}H_3)_2$; $\mathit{C}H_3CH_2NC$	N$\mathit{C}H_3$; $CH_3\mathit{C}H_2NC$	N($\mathit{C}H_2CH_3)_2$; N(Me)$\mathit{C}H_2CH_3$	Tp′*C*H	Tp′*C*Me	EtN*C*	W≡*C*	solvent; *T* (°C)
2a	12.3; 12.7; 14.4; 19.5 (1:2:1:2)	26.3	–	31.3	43.0	107.2; 107.6 (2:1)	143.8; 148.3; 154.6; 156.4 (1:2:1:2)	–	267.1 ^1J(WC) = 240.6	CD_2Cl_2; +20
2b	12.3; 12.7; 14.4; 19.4 (1:2:1:2)	–	26.5	–	39.4	107.1; 107.6 (2:1)	143.8; 148.4; 154.6; 156.7 (1:2:1:2)	–	266.5 ^1J(WC) = 241.7	CD_2Cl_2; +20
3a	12.3; 12.5; 17.1; 20.5 (1:2:1:2)	28.0	–	32.1	40.3	106.5; 107.8 (2:1) (1:2:1:2)	144.7; 149.1; 156.4; 158.8	–	265.5	CD_2Cl_2; +20
3b	12.3; 12.4; 17.0; 20.3 (1:2:1:2)	–	31.5	–	36.0	106.4; 107.8 (2:1)	144.7; 149.1; 156.4; 159.3 (1:2:1:2)	–	263.8	CD_2Cl_2; +20
4a	12.6; 12.7; 16.1; 17.4 (1:2:1:2)	14.0	16.9	36.0; 43.8 [a]	47.0	105.9; 106.2 (2:1)	143.0; 143.2; 151.3; 151.5 (2:1:2:1)	222.3 ^1J(WC) = 164.8	243.1 ^1J(WC) ≐ 231.9	C_6D_6; +20
4b	12.6; 12.7; 16.1; 17.3 (1:2:1:2)	–	15.0; 17.0 [b]	43.8	44.3	105.9; 106.2 (2:1)	143.0; 143.2; 151.3; 151.4 (2:1:1:2)	222.6 ^1J(WC) = 165.0	242.6 ^1J(WC) = 230.9	C_6D_6; +20
5a	12.5; 12.6; 13.0; 15.3; 15.4; 17.6	13.4	13.8; 14.4 [b]	37.9; 40.2 [a]	45.9 [c]; 49.0	106.1; 106.8; 106.9	145.5; 146.6; 150.7; 152.1 152.3 (2:1:1:1:1)	153.1	260.7	CD_2Cl_2; −60
5b	12.7; 13.1; 15.5; 17.8 (2:1:2:1)	–	13.9; 14.6 [b]	40.4	45.9	106.4; 107.0 (1:2)	145.6; 146.6; 150.9; 152.4 (2:1:1:2)	153.5	261.5 [d]	CD_2Cl_2; −20

[a] Methylene-carbon resonance. [b] Resonance of the ethyl isocyanide ligand. [c] Resonance of the diethylaminocarbyne ligand. [d] The two carbyne-carbon resonances are by accident coincident.

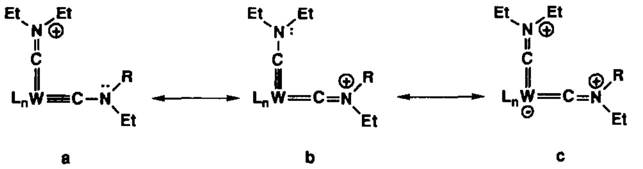

Fig. 7. Resonance forms for the metal–carbyne bonds in the bis-aminocarbyne complexes **5a** and **5b**.

describe the metal–carbyne bonding in **5a** and **5b**, since only six electrons are present in the metal–ligand π-orbitals and eight electrons would be required to form two independent metal–carbon triple bonds.

The $\nu(\mathrm{C_{carbyne}} \overset{\cdot\cdot}{-} \mathrm{N})$ absorptions of the bis-aminocarbyne complexes **5a** and **5b** appear at higher frequency than those of the mono-aminocarbyne precursors **4a** and **4b** (Table 1). A similar trend has been previously observed for analogous Cp*-substituted compounds [*e.g.*, $\nu(\mathrm{C} \overset{\cdot\cdot}{-} \mathrm{N})$ of $\mathrm{Cp^*({}^tBuNC)_2W{\equiv}CNEt_2}$ in n-pentane: 1506 cm^{-1}; $\nu(\mathrm{C} \overset{\cdot\cdot}{-} \mathrm{N})$ of $\mathrm{\{Cp^*({}^tBuNC)W[\overset{\cdot\cdot}{\equiv}CN({}^tBu)Et](\overset{\cdot\cdot}{\equiv}CNEt_2)\}BF_4}$ in $\mathrm{CH_2Cl_2}$: 1601, 1522 cm^{-1}] [6a] and can be explained by the considerable decrease in electron density occurring at the metal centre upon ethylation of **4a** and **4b**. This decrease is accompanied by a dramatic shift of the $\nu(\mathrm{C{\equiv}NEt})$ absorptions by more than 300 cm^{-1} to higher wavenumbers on going from the electron-rich mono-aminocarbyne complexes **4a** and **4b** to their ethylation products **5a** and **5b** (Table 1).

3.2. *^{1}H and ^{13}C NMR spectra*

Additional support for the assigned structures is given by the ^{1}H and ^{13}C NMR spectra (Tables 2 and 3). Thus, the ^{1}H NMR spectra of the mono-aminocarbyne complexes **2a**–**4b** display one triplet resonance for the methyl protons and one quartet resonance for the methylene protons of the ethyl groups in the aminocarbyne ligand, indicating C_s molecular symmetry and rapid rotation of the amino group about the $\mathrm{C_{carbyne}}$–N bond on the NMR time scale. Further evidence for the C_s symmetry of these compounds is given by the 2/1 pattern of singlet resonances observed for the methyl and ring protons of the pyrazol-1-yl groups (Table 2). Similarly, the ^{1}H NMR spectrum of the bis-aminocarbyne complex **5b** displays only one triplet resonance for the methyl protons of the diethylaminocarbyne ligands at δ 1.29 and two singlet resonances for the ring protons of the Tp′ ligand at δ 5.93 and 5.95 (ratio 2/1), indicating a rapid equilibration of the three possible conformers due to fast rotation of the amino groups around the $\mathrm{C_{carbyne}}$–N bonds (see results and discussion). In comparison, a 1/1/1 pattern of singlet resonances is observed for the methyl and ring protons of the pyrazol-1-yl groups in **5a**, suggesting the presence of a chiral metal centre ($\mathrm{C_1}$ molecular symmetry). Evidence for a fast rotation of the amino groups around the $\mathrm{C_{carbyne}}$–N bonds in **5a** is given by the one triplet resonance observed for the methyl protons of the diethylaminocarbyne ligand at δ 1.29 (Table 2).

The symmetry plane of **4a** and **4b** does not bisect the methylene groups of the two equivalent ethyl isocyanide ligands. Therefore these methylene protons are diastereotopic giving rise to two doublet of quartets at δ 3.42 and 3.48 (**4a**) and δ 3.45 and 3.51 (**4b**) (Table 2). For the same reason the methylene protons of the equivalent diethylaminocarbyne ligands in **5b** are diastereotopic giving rise to two doublet of quartets at δ 3.42 and 3.57.

Notably, extremely low-field resonances are observed for the methylene protons of the d^3 aminocarbyne complexes **2a**–**3b** (δ 6.55–7.94) (the carbyne fragment is considered in the monocarbyne complexes **2a**–**3b** as a neutral 3e-donor ligand giving the tungsten centre a formal d^3 electron configuration) (Table 2). These chemical shifts are the largest so far reported for terminal aminocarbyne ligands. In comparison, the methylene proton resonances of the d^3 aminocarbyne complexes $\mathrm{Cp^*(X)_2(CO)W{\equiv}CNEt_2}$ appear at considerably higher field [X = Br: $\delta(\mathrm{C}H_2)$ 3.47, 3.50 ($\mathrm{CD_2Cl_2}$, 0°C); X = I: $\delta(\mathrm{C}H_2)$ 3.46, 3.53 ($\mathrm{CD_2Cl_2}$, 25°C)] [10b].

The ^{13}C NMR spectra also support the proposed structures for **2a**–**5b** (Table 3). Thus, the d^3 aminocarbyne complexes **2a**–**3b** are distinguished by a carbyne-carbon resonance at δ 263.8–267.1, which appears at lower field than that of the d^5 aminocarbyne complexes **4a** (δ 243.1) and **4b** (δ 242.6). A similar change in the chemical shift of the carbyne-carbon has been previously observed on going from d^3 to d^5 aminocarbyne complexes containing a Cp or Cp* ligand [6a,10c,16b, 16c]. In addition, the aminocarbyne complexes **4a** and **4b** exhibit two extremely low-field resonances for the isocyanide-carbons at δ 222.3 and 222.6, respectively. Comparable low-field resonances have been observed also for other electron-rich isocyanide complexes of Group VI metals [*e.g.*, $\mathrm{Cp_2WCNEt}$: δ_{CNEt}: 244.0; $\mathrm{Cp^*(EtNC)_2W{\equiv}CNEt_2}$: δ_{CNEt} 223.9; $\mathrm{Cp^*(CO)(EtNC)W{\equiv}CNEt_2}$: δ_{CNEt} 209.7] [6a,17]. The deshielding of the isocyanide-carbon results from the strong metal–isocyanide back bonding in these compounds [18].

The carbyne-carbon resonance of **2a**–**4b** displays tungsten satellites due to coupling with the ^{183}W nucleus. The ^1J(WC) coupling constants of the six-coordinate d^3 aminocarbyne complexes **2a** (240.6 Hz) and **2b** (241.7 Hz) are larger than those of seven-coordinate d^3 aminocarbyne complexes containing a Cp* ligand [*e.g.*, $\mathrm{Cp^*(Br)_2(CO)W{\equiv}CNEt_2}$: ^1J(WC) = 206.3 Hz;

Cp*(Br)$_2$(^{t}BuNC)W≡CNEt$_2$: ^1J(WC) = 219.7 Hz; [Cp*(Br)(PMe$_3$)$_2$W≡CNEt$_2$]Br: ^1J(WC) = 207 Hz] [19] and indicate, in full agreement with the IR spectra, a stronger metal–carbyne backbonding in the Tp′ complexes. In comparison, The ^1J(WC) coupling constants of the d^5 aminocarbyne complexes **4a** (231.9 Hz) and **4b** (230.9 Hz) are smaller than those of analogous Cp and Cp* substituted derivatives [*e.g.*, Cp*(CO)$_2$W≡CN(Et)CH$_2$SiMe$_3$: ^1J(WC) = 235.6 Hz; Cp(CO)(EtNC)W≡CNEt$_2$: ^1J(WC) = 240.5 Hz; Cp*(CO)(MeNC)W≡CNEt$_2$: ^1J(WC) = 241.6 Hz] [19].

The bis-aminocarbyne complexes **5a** and **5b** are also distinguished by low-field carbyne-carbon resonances at δ 260.7 and 261.5, respectively (Table 3). These resonances appear at an even lower field than those of the mono-aminocarbyne precursors **4a** (δ 243.1) and **4b** (δ 242.6). The same trend is observed for analogous Cp* derivatives [*e.g.*, Cp*(EtNC)$_2$W≡CNEt$_2$: δ 257.9 (C$_6$D$_6$, 20°C); [Cp*(EtNC)W(≡CNEt$_2$)$_2$]BF$_4$: δ 276.2 (CD$_2$Cl$_2$, −80°C)] and offers a powerful spectroscopic tool for distinguishing between mono-aminocarbyne, bis-aminocarbyne complexes and ynediamine coupling products (the latter show resonances for the alkyne-carbons at δ 180–210) [6].

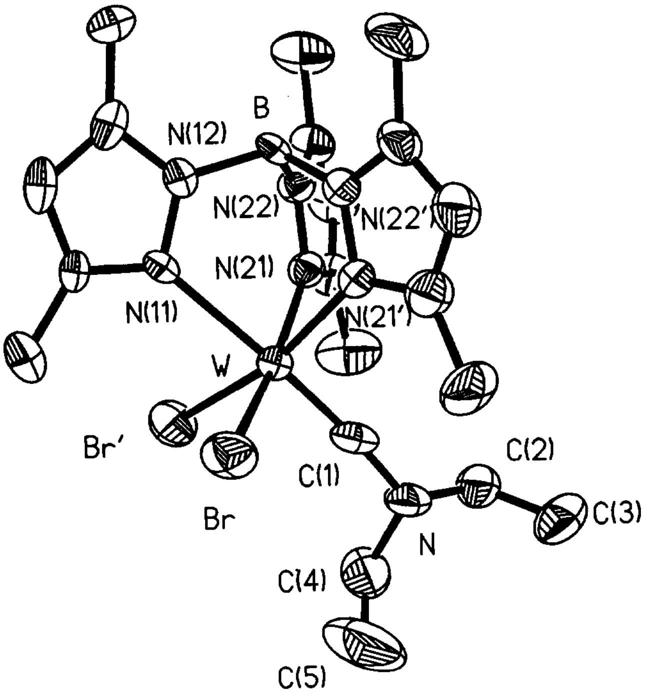

Fig. 8. ORTEP plot of **2b** with thermal ellipsoids drawn at the 50% probability level. Hydrogen atoms are omitted for clarity.

3.3. *Crystal structure of* 2b

The molecular structure of **2b** was determined by a single crystal X-ray diffraction study. A SCHAKAL plot of a single molecule with the atom numbering scheme adopted is given in Fig. 8. Selected bond lengths and angles are listed in Table 4.

The distorted octahedral complex has C_s symmetry, the mirror plane being defined by the tungsten centre, the carbyne-carbon, the amino-nitrogen and the N(11), N(12), C(13), C(14), C(15), C(16) and C(17) atoms of one pyrazol-1-yl group (Fig. 8).

The aminocarbyne ligand is linearly coordinated to the tungsten centre as indicated by the W–C$_1$–N angle of 174.5(5)° and has a strong *trans* influence as reflected in the W–N(11) bond of 234.0(5) pm, which is considerably longer than the W–N(21) and W–N(21)′ bonds that are *trans* to the bromo ligands [213.1(3) pm].

TABLE 4. Selected bond lengths (pm) and bond angles (°) with estimated standard deviations for **2b**

W–Br	252.74(5)	N(21)–W–Br′	89.80(8)
W–Br′	252.74(5)	N(11)–W–N(21)	84.7(1)
W–C(1)	176.3(8)	N(11)–W–C(1)	177.3(2)
W–N(11)	234.0(5)	N(21)–W–C(1)	97.4(2)
W–N(21)	213.1(3)	Br–W–Br′	98.77(2)
W–N(21)′	213.1(3)	C(1)–W–Br	92.5(1)
C(1)–N	134.5(8)	W–C(1)–N	174.5(5)
C(2)–N	144.3(9)	C(1)–N–C(2)	125.4(7)
C(4)–N	157(1)	C(1)–N–C(4)	114.8(6)
N(11)–W–Br	85.73(8)	C(2)–N–C(4)	119.1(7)
N(21)–W–Br	166.63(9)		

The W–C$_{\text{carbyne}}$ bond length of 176.3(8) pm is similar to those reported for other carbonyl-free d^3 tungsten carbyne complexes (Schrock-type alkylidyne complexes), such as [(^{t}BuO)$_2$(μ-O^{t}Bu)W≡CNMe$_2$]$_2$ [W–C$_{\text{carbyne}}$ = 175(2) and 177(2) pm] [20a], {[η^5-C$_5$Me$_4$(^{t}Bu)](I)W≡C^{t}Bu}$_2$(μ-N$_2$H$_2$) [W–C$_{\text{carbyne}}$ = 176.9(8) pm] [20b] and (^{t}BuO)$_3$W≡CPh [W–C$_{\text{carbyne}}$ = 175.8(5) pm] [20c]. It is, however, significantly smaller than that of the carbonyl-containing d^3 aminocarbyne complex (η^5-C$_5$Me$_4$Et)(Br)$_2$(CO)W≡CNEt$_2$ [W–C$_{\text{carbyne}}$ = 185(1) pm] [21a], supporting, along with the IR and ^{13}C NMR data, the argument for stronger tungsten–carbyne back bonding in the Tp′ compound. The W–C$_{\text{carbyne}}$ bond of **2b** is also shorter than those found in d^5 tungsten aminocarbyne complexes (Fischer-type carbyne complexes) due to differences in the ionic radii of W$^{\text{III}}$ and W$^{\text{I}}$ centres [*e.g.*, *trans*-Br(CO)$_4$W≡CNCPh$_2$: W–C$_{\text{carbyne}}$ = 187.8(5) pm; (CO)$_5$CrPPh$_2$(CO)$_2$(2.2′-bipy)W≡CNEt$_2$: W–C$_{\text{carbyne}}$ = 187.7(8) pm] [21b, c].

The C$_{\text{carbyne}}$–N bond of 134.5(8) pm is intermediate in length between that expected for a C(sp^2)–N(sp^2) single (144 pm) and a C(sp^2)=N(sp^2) double bond (127 pm) [22], reflecting as in other aminocarbyne complexes a high degree of π bonding between the carbyne-carbon and the amino-nitrogen [2]. Further evidence for this is given by the planar arrangement of the atoms C_1, N, C_2 and C_4 (amino plane) or the sum of angles around N (359.3°) consistent with a sp^2-hybridization of the nitrogen atom.

4. Experimental section

Standard Schlenk procedures were used for all syntheses and sample manipulations. The solvents were dried by standard methods (n-pentane, Et_2O and THF over Na/benzophenone; CH_2Cl_2 over P_2O_5 and Na/Pb alloy), distilled under nitrogen and stored over 4 Å molecular sieves prior to use. All column chromatography was performed on a silica support (Merck, activity I, 0.063–0.2 mm, dried *in vacuo* and stored under nitrogen) as the stationary phase in a thermostated column of 45 cm length and 2.0 cm diameter.

Elemental analyses were performed by the Microanalytical Laboratory of this department. IR spectra were recorded on a Nicolet 5DX and a Perkin Elmer 1650 FT spectrophotometer. ^1H and ^{13}C NMR spectra were recorded in dry deoxygenated methylene-d_2-chloride or benzene-d_6 on a JEOL-JMX-GX 400 instrument. Chemical shifts were referenced to residual solvent signals (CD_2Cl_2, δ_H 5.32 and δ_C 53.8 ppm; C_6D_6, δ_H 7.15 and δ_C 128.0 ppm). Mass spectra were obtained with Varian MAT 311A and MAT 90A spectrometers; m/z values are relative to the ^{184}W, ^{11}B and ^{79}Br isotopes. Complexes **1a** and **1b** were prepared as described previously [9].

4.1. Preparations

4.1.1. Tp'(Br)$_2$W≡CN(Me)Et (2a)

A solution of 0.059 ml (1.15 mmol) of Br_2 in 20 ml of CH_2Cl_2 was added dropwise at −80°C to a yellow solution of 690 mg (1.14 mmol) of **1a** in 50 ml of CH_2Cl_2. The reaction mixture was then allowed to warm to room temperature and stirred for 2 h. Evolution of gas (CO) and a change from yellow to blue were observed. Completion of the reaction was confirmed by IR spectroscopy (disappearance of the ν(CO) absorptions of the starting material at 1936 and 1833 cm^{-1}). The solvent was then removed *in vacuo* and the residue purified by column chromatography on silica at 0°C. The product was eluted with CH_2Cl_2/Et_2O (2/1), the blue eluate concentrated under vacuum and n-pentane added to bring about complete precipitation of **2a**. The supernatant solution was decanted off and the precipitate dried *in vacuo*. Blue solid. M.p.: 243°C (dec.). Yield: 620 mg (77%). Found: C, 32.02; H, 4.33; Br, 23.05; N, 13.45; W, 25.07. $C_{19}H_{30}BBr_2N_7W$ (710.96) calc.: C, 32.10; H, 4.25; Br, 22.48; N, 13.79; W, 25.86%. EI-MS (70 eV): m/z 709 (M^+), 639 ($[M-CN(Me)Et]^+$) (base peak), 560 ($[M-CN(Me)Et-Br]^+$), 543 ($[M-CN(Me)Et-3{,}5\text{-dimethylpyrazole}]^+$).

4.1.2. Tp'(Br)$_2$W≡CNEt$_2$ (2b)

A yellow solution of 250 mg (0.40 mmol) of **1b** in 20 ml of CH_2Cl_2 was treated at −80°C with a solution of 0.021 ml (0.41 mmol) of Br_2 in 10 ml of CH_2Cl_2. The reaction mixture was then warmed to room temperature and stirred for 2 h until reaction was complete (IR monitoring). The resulting blue solution was evaporated to dryness and the residue purified as described for the synthesis of **2a** to give complex **2b** as a blue solid. M.p.: 230°C (dec.). Yield: 240 mg (82%). Found: C, 32.74; H, 4.37; Br, 22.30; N, 13.59; W, 25.41. $C_{20}H_{32}BBr_2N_7W$ (724.99) calc.: C, 33.13; H, 4.45; Br, 22.04; N, 13.52; W, 25.36%. EI-MS (70 eV): m/z 723 (M^+), 694 ($[M-Et]^+$), 639 ($[M-Et-CNEt]^+$), 560 ($[M-Et-CNEt-Br]^+$), 543 ($[M-Et-CNEt-3{,}5\text{-dimethylpyrazole}]^+$).

4.1.3. Tp'(I)$_2$W≡CN(Me)Et (3a)

A solution of 300 mg (0.49 mmol) of **1a** in 40 ml of CH_2Cl_2 was treated at −80°C with a solution of 150 mg (0.59 mmol) of I_2 in 15 ml of CH_2Cl_2. The reaction mixture was then allowed to warm to room temperature and refluxed for 13 h. During this time evolution of gas (CO) was observed and the colour of the solution changed from yellow to green. After all of the starting material had been consumed (IR monitoring as in the synthesis of **2a**) the solvent was removed *in vacuo*, and the residue purified by column chromatography on silica at −5°C. Excess iodine was first removed with Et_2O/n-pentane (1/3) and the product then eluted with CH_2Cl_2/Et_2O (1/1). The green eluate was concentrated under vacuum and n-pentane was added to bring about complete precipitation of **3a**. The supernatant solution was decanted off and the precipitate dried *in vacuo*. Olive-green solid. M.p.: 240°C (dec.). Yield: 320 mg (80%). Found: C, 28.95; H, 3.75; I, 31.06; N, 12.41; W, 22.66. $C_{19}H_{30}BI_2N_7W$ (804.96) calc.: C, 28.35; H, 3.76; I, 31.53; N, 12.18; W, 22.84%. EI-MS (70 eV): m/z 805 (M^+) (base peak), 735 ($[M-CN(Me)Et]^+$), 608 ($[M-CN(Me)Et-I]^+$), 481 ($[M-CN(Me)Et-2\,I]^+$).

4.1.4. Tp'(I)$_2$W≡CNEt$_2$ (3b)

A solution of 650 mg (1.05 mmol) of **1b** in 40 ml of CH_2Cl_2 was treated at −80°C with a solution of 292 mg (1.15 mmol) of I_2 in 15 ml of CH_2Cl_2. The reaction mixture was then allowed to warm to room temperature and refluxed for 23 h. The resulting green solution was worked up as described for the synthesis of **3a** to give complex **3b** as an olive-green, microcrystalline solid. M.p.: 235°C (dec.). Yield: 740 mg (86%). Found:

C, 29.56; H, 3.90; I, 29.07; N, 11.86; W, 23.34. $C_{20}H_{32}BI_2N_7W$ (818.98) calc.: C, 29.33; H, 3.94; I, 30.99; N, 11.97; W, 22.45%. EI-MS (70 eV): *m/z* 819 (M^+) (base peak), 735 ($[M - CNEt_2]^+$), 608 ($[M - CNEt_2 - I]^+$), 481 ($[M - CNEt_2 - 2\,I]^+$).

4.1.5. $Tp'(EtNC)_2W{\equiv}CN(Me)Et$ (4a)

A green solution of 170 mg (0.21 mmol) of **3a** in 20 ml of THF was treated at −80°C with 0.032 ml (0.43 mmol) EtNC and 0.24 ml of 0.85% (w/w) Na/Hg (1.19 mmol Na) and the reaction mixture warmed to room temperature and stirred for 6 h. The grey precipitate, consisting of NaI and Na/Hg, was allowed to settle and the supernatant yellow-brown solution filtered. The filtrate was evaporated to dryness and the residue freed from NaI by extraction with Et_2O/n-pentane (1/2) and filtration. The filtrate was evaporated to dryness under vacuum and the residue recrystallized twice from a minimum amount of n-pentane to give complex **4a** as a yellow, microcrystalline solid. Yield: 100 mg (72%). $C_{25}H_{40}BN_9W$ (661.31). EI-MS (70 eV): *m/z* 661 (M^+), 551 ($[M - 2\,EtNC]^+$), 481 ($[M - 2EtNC - CN(Me)Et]^+$).

4.1.6. $Tp'(EtNC)_2W{\equiv}CNEt_2$ (4b)

A green solution of 290 mg (0.35 mmol) of **3b** in 20 ml of THF was treated at −80°C with 0.061 ml (0.82 mmol) EtNC and 0.32 ml of 0.85% (w/w) Na/Hg (1.59 mmol Na) and the reaction mixture warmed to room temperature and stirred for 3 h. The resulting suspension was worked up as described for the synthesis of **4a** to give complex **4b** as a yellow, microcrystalline solid. Yield: 145 mg (61%). $C_{26}H_{42}BN_9W$ (675.34). EI-MS (70 eV): *m/z* 675 (M^+), 591 ($[M - CN(Me)Et]^+$), 565 ($[M - 2\,EtNC]^+$), 481 ($[M - 2\,EtNC - CN(Me)Et]^+$).

4.1.7. $\{Tp'(EtNC)W[\doteq CN(Me)Et][\doteq CNEt_2]\}BF_4$ (5a)

140 mg (0.21 mmol) of **4a** were dissolved in 20 ml of precooled (−80°C) CH_2Cl_2 and the solution treated at −80°C with a solution of 38 mg (0.20 mmol) of $[Et_3O]BF_4$ in 10 ml of CH_2Cl_2. The reaction mixture was warmed to −30°C and stirred for 1 h until reaction was complete (IR monitoring). The resulting yellow-green solution was then reduced in volume under vacuum and Et_2O/n-pentane (1/2) was added to precipitate complex **5a**. Recrystallization from CH_2Cl_2 and Et_2O/n-pentane was repeated twice to give complex **5a** as a yellow solid. Yield: 140 mg (85%). Found: C, 41.40; H, 5.76; N, 16.10; W, 23.22. $C_{27}H_{45}B_2F_4N_9W$ (777.18) calc.: C, 41.73; H, 5.84; N, 16.22; W, 23.66%.

4.1.8. $[Tp'(EtNC)W(\doteq CNEt_2)_2]BF_4$ (5b)

A solution of 140 mg (0.21 mmol) of **4b** in 20 ml of precooled (−80°C) CH_2Cl_2 was treated at −80°C with a solution of 38 mg (0.20 mmol) of $[Et_3O]BF_4$ in 10 ml of CH_2Cl_2. The reaction mixture was warmed to −30°C and stirred for 1 h. Completion of the reaction was confirmed by IR spectroscopy (disappearance of the two $\nu(C{\equiv}NEt)$ and the $\nu(C_{carbyne} \doteq N)$ absorption of the starting material at 1880w, 1787s and 1499m cm^{-1}, respectively). The resulting solution was worked up as described above for the isolation of **5a** to afford complex **5b** as a yellow solid. Yield: 150 mg (91%). Found: C, 42.06; H, 5.71; N, 15.62; W, 22.99. $C_{28}H_{47}B_2F_4N_9W$ (791.21) calc.: C, 42.51; H, 5.99; N, 15.93; W, 23.24%.

4.2. MO calculations

The MO calculations reported in this work are of the Extended Hückel type [23]. A weighted H_{ij}-formula was used throughout for computing the off-diagonal matrix elements [24]. Atomic parameters for H, C and N were standard ones [23]. The tungsten atomic wavefunctions and VSIP values were taken from earlier work [25]. The model geometries for the CpW(CO)-complexes employed the following structural data: Cp-ring: C–C = 140 pm, C–H = 108 pm, C_5H_5 of local D_{5h} symmetry; W–Cp(centre) = 206 pm; $W{-}C_{CO}$ = 190 pm, C–O = 125 pm, Cp(centre)–W–C_{CO} = 143.8°; W–$C_{carbyne}$ = 203.9 pm, C–H = 108 pm, C–N = 133 pm, N–H = 100 pm, C–N–H = 120°, H–N–H = 120°. The $W(CO)(CR)_2$ sub-unit in the bis-carbyne complexes was taken as an octahedral fragment (all C–W–C angles = 90°). For calculating the energy surfaces E(α, β) the angles were varied independently from α = 180° to 100° and from β = 100° to 30° for both the CH and the CNH_2 ligands. Single point calculations (for **A–G**) used α = 180° and β = 90° for the bis(carbyne) complexes and α = 148.58° and β = 37.16° for the alkyne isomers, making the C–C bond in the latter 130 pm and the N–C–C angle in the ynediamine ligand 140°, similar to the minima on the E = E(α, β) energy surfaces.

4.3. Crystal structure determination of 2b

Suitable crystals were obtained as blue prisms by slow evaporation of a CH_2Cl_2 solution of **2b**. Complex **2b** crystallizes in the orthorhombic space group *Pnma* (Intern. Tables No. 62). Unit cell dimensions were determined by centring and least squares refinement of 25 reflections at high θ angles ($a = 2420.2(2)$, $b = 1279.86(7)$, $c = 825.20(9)$ pm; $V = 2556 \times 10^6$ pm^3, Z = 4, $\rho_{calc.} = 1.884$ g/cm^3). Data collection was performed on a CAD4 diffractometer with graphite monochromated Mo Kα radiation ($\lambda = 71.073$ pm) at ambient temperature (23 ± 3°C). Intensity data for 4930 reflections in the range $2° \leq 2\theta \leq 50°$ ($+h$, $\pm k$, $+l$) were collected by ω-scan with a scan width of $(0.90 + 0.30 \tan \theta)°$ ± 25% for background determination.

Maximal scan time was 60 s. The intensity data were corrected for Lorentz and polarization effects and for absorption (empirical correction, 8 reflections, $\mu = 77.34\ \text{cm}^{-1}$, transmission ranges 0.4330–0.9989). During data collection no significant decay of three intensity control reflections was observed. After merging, 2183 and 2187 unique reflections ($I \geq 0.0$) were used in the refinement. The structure was solved by the Patterson method (SHELXS-86) [26] and subsequent least-squares cycles and difference Fourier syntheses. All non hydrogen atoms were refined with anisotropic displacement parameters. Hydrogen atoms were placed in idealized positions (d(C–H), d(B–H) = 95 pm) and were included in the structure factor calculation but not refined (176 parameters). Refinement minimized the function $\Sigma w(|F_o| - |F_c|)^2$, where $w = 1/\sigma^2$ and converged yielding R values of $R(F) = 0.040$ and $R_w(F) = 0.021$. In the final stages of the refinement data were corrected for secondary extinction effects ($\epsilon = 2.29425 \times 10^{-8}$). Residual electron density maxima and minima were $+1.01$ and $-0.949\ \text{e}/\text{Å}^3$ at the tungsten atom. Atomic scattering parameters were taken from ref. 27. Anomalous dispersion effects were included for all non hydrogen atoms [28]. Calculations were performed using the SDP [29] and STRUX-IV [30] systems on a MicroVAX 3100 computer. Plots of the structure were made using the program ORTEP [31]. Further details of the crystal structure determination are available on request from the Fachinformationszentrum Karlsruhe, Gesellschaft für wissenschaftlich-technische Information mbH, D-76344 Eggenstein-Leopoldshafen, Germany, on quoting the depository number CSD-57620, the names of the authors and the journal citation.

Acknowledgments

We thank Professor W.A. Herrmann for providing institute facilities, the Volkswagen Stiftung, the Deutsche Forschungsgemeinschaft and the Fonds der Chemischen Industrie for financial support, Mr. M. Barth, Ms. I. Liss and Ms. A. Fuss for elemental analyses, Professor F.R. Kreissl, Ms. R. Dumitrescu and Ms. I. Werner for the mass spectra and Dr. H.B. Friedrich for proof-reading the manuscript.

References and notes

1 (a) R. Hoffmann, C.N. Wilker and O. Eisenstein, *J. Am. Chem. Soc.*, *104* (1982) 632; (b) C.N. Wilker, R. Hoffmann and O. Eisenstein, *Nouv. J. Chim.*, *7* (1983) 535.

2 H. Fischer, P. Hofmann, F.R. Kreissl, R.R. Schrock, U. Schubert and K. Weiss, *Carbyne Complexes*, VCH, Weinheim, 1988. Note that the electron count in this work differs from that in ref. 2, where the CH moieties were considered as 2e donors, making the coupling reaction allowed for a d^4 to d^6 metal centre. We prefer here the picture of the carbyne ligands as 3e donors, because this leads to a consistent electron count in the $[CpW(CO)]^+$ fragment for both the bis-carbyne and the alkyne complexes, where a neutral alkyne ligand is the more "natural" choice.

3 P. Hofmann, in A. Veillard (ed.), *Quantum Chemistry: The Challenge of Transition Metals and Coordination Chemistry*, NATO ASI Series, Vol. 176, D. Reidel Publishing Co., Amsterdam, 1986, p. 253.

4 (a) G.A. McDermott and A. Mayr, *J. Am. Chem. Soc.*, *109* (1987) 580; (b) A. Mayr, C.M. Bastos, N. Daubenspeck and G.A. McDermott, *Chem. Ber.*, *125* (1992) 1583.

5 (a) J. Chatt, A.J.L. Pombeiro, R.L. Richards, G.H.D. Royston, K.W. Muir and R. Walker, *J. Chem. Soc., Chem. Commun.*, (1975) 708; (b) J. Chatt, A.J.L. Pombeiro and R.L. Richards, *J. Chem. Soc., Dalton Trans.*, (1980) 492; (c) A.J.L. Pombeiro and R.L. Richards, *Coord. Chem. Rev.*, *104* (1990) 13.

6 (a) A.C. Filippou, W. Grünleitner, C. Völkl and P. Kiprof, *Angew. Chem.*, *103* (1991) 1188; *Angew. Chem. Int. Ed. Engl.*, *30* (1991) 1167; (b) A.C. Filippou, C. Völkl, W. Grünleitner and P. Kiprof, *J. Organomet. Chem.*, *434* (1992) 201.

7 (a) A.C. Filippou and W. Grünleitner, *Z. Naturforsch. B*, *44* (1989) 1023; (b) A.C. Filippou, *Polyhedron*, *9* (1990) 727; (c) A.C. Filippou, C. Völkl, W. Grünleitner and P. Kiprof, *Angew. Chem.*, *102* (1990) 224; *Angew. Chem. Int. Ed. Engl.*, *29* (1990) 207; (d) A.C. Filippou, C. Völkl, W. Grünleitner and P. Kiprof, *Z. Naturforsch. B*, *45* (1990) 351; (e) A. Mayr and C.M. Bastos, *J. Am. Chem. Soc.*, *112* (1990) 7797; (f) A. Mayr and C.M. Bastos, *Prog. Inorg. Chem.*, *40* (1992) 1.

8 (a) C.T. Lam, P.W.R. Corfield and S.J. Lippard, *J. Am. Chem. Soc.*, *99* (1977) 617; (b) C.M. Giandomenico, C.T. Lam and S.J. Lippard, *J. Am. Chem. Soc.*, *104* (1982) 1263; (c) R.N. Vrtis and S.J. Lippard, *Isr. J. Chem.*, *30* (1990) 331; (d) A.C. Filippou and W. Grünleitner, *J. Organomet. Chem.*, *393* (1990) C10; (e) A.C. Filippou and W. Grünleitner, *Z. Naturforsch. B*, *46* (1991) 216; (f) E.M. Carnahan and S.J. Lippard, *J. Chem. Soc., Dalton Trans.*, (1991) 699; (g) E.M. Carnahan, J.D. Protasiewicz and S.J. Lippard, *Acc. Chem. Res.*, *26* (1993) 90.

9 A.C. Filippou, C. Wagner, E.O. Fischer and C. Völkl, *J. Organomet. Chem.*, *438* (1992) C15.

10 (a) A.C. Filippou and E.O. Fischer, *J. Organomet. Chem.*, *341* (1988) C35; (b) A.C. Filippou and E.O. Fischer, *J. Organomet. Chem.*, *349* (1988) 367; (c) A.C. Filippou, E.O. Fischer and W. Grünleitner, *J. Organomet. Chem.*, *386* (1990) 333.

11 (a) J.A. McCleverty, *Chem. Soc. Rev.*, *12* (1983) 331; (b) C.G. Young, S.A. Roberts, R.B. Ortega and J.H. Enemark, *J. Am. Chem. Soc.*, *109* (1987) 2938; (c) A.S. Gamble, P.S. White and J.L. Templeton, *Organometallics*, *10* (1991) 693.

12 (a) P. Hofmann and M. Padmanabhan, *Organometallics*, *2* (1983) 1273; (b) J. Silvestre, M.J. Calhorda, R. Hoffmann, P.O. Stoutland and R.G. Bergman, *Organometallics*, *5* (1986) 1841.

13 This is a simple consequence of A being an "octahedral" 18e complex, the distortion of which will cost appreciable energy as long as it has not yet reached a 16e stage by CH/CH coupling.

14 The $E = E(\alpha, \beta)$ coupling energy surface was calculated for the C to F least motion process keeping the NH_2 groups in plane throughout. Simultaneous optimization of their relative rotational orientation does not alter the basic features of the energetic course of the alkyne formation.

15 K. Ackermann, P. Hofmann, F.H. Köhler, H. Kratzer, H. Krist, K. Öfele and H.R. Schmidt, *Z. Naturforsch. B*, *38* (1983) 1313.

16 (a) A.C. Filippou, E.O. Fischer and R. Paciello, *J. Organomet Chem.*, *347* (1988) 127; (b) A.C. Filippou, *Polyhedron*, *8* (1989) 1285; (c) A.C. Filippou and W. Grünleitner, *Z. Naturforsch. B*, *44*

(1989) 1572; (d) A.C. Filippou and E.O. Fischer, *J. Organomet. Chem., 382* (1990) 143.

17 (a) A.C. Filippou and W. Grünleitner, *J. Organomet. Chem., 407* (1991) 61; (b) A.C. Filippou, A.R. Dias, A.M. Martins and C.C. Romao, *J. Organomet. Chem.*, *455* (1993) 129.

18 D.L. Cronin, J.R. Wilkinson and L.J. Todd, *J. Magn. Res., 17* (1975) 353.

19 (a) W. Grünleitner, *Dissertation,* TU München, 1991; (b) B. Lungwitz, *Diplomarbeit,* TU München, 1992.

20 (a) M.H. Chisholm, J.C. Huffman and N.S. Marchant, *J. Am. Chem. Soc., 105* (1983) 6162; (b) M.R. Churchill, Y.-J. Li, L. Blum and R.R. Schrock, *Organometallics, 3* (1984) 109; (c) F.A. Cotton, W. Schwotzer and E.S. Shamshoum, *Organometallics, 3* (1984) 1770.

21 (a) A.C. Filippou and B. Lungwitz, unpublished results; (b) H. Fischer, F. Seitz and J. Riede, *J. Chem. Soc., Chem. Commun.*, (1985) 537; (c) A.C. Filippou, E.O. Fischer, H.G. Alt and U. Thewalt, *J. Organomet. Chem., 326* (1987) 59.

22 (a) M. Burke-Laing and M. Laing, *Acta Crystallogr. B, 32* (1976) 3216; (b) I. Hargittai and R. Seip, *Acta Chem. Scand. A, 30* (1976) 540.

23 R. Hoffmann, *J. Chem. Phys., 39* (1963) 1397; R. Hoffmann, *J. Chem. Phys., 40* (1964) 2475, 2480 and 2745.

24 J.H. Ammeter, H.-B. Bürgi, J.C. Thibeault and R. Hoffmann, *J. Am. Chem. Soc., 100* (1978) 3686.

25 P. Hofmann, M. Hämmerle and G. Unfried, *New. J. Chem., 15* (1991) 769.

26 G.M. Sheldrick, SHELXS-86, Universität Göttingen, Germany, 1986.

27 D.T. Cromer and J.T. Waber, *International Tables of Crystallography, Vol. 4*, Table 2.2B, Kynoch Press, Birmingham, UK, 1974.

28 D.T. Cromer, *International Tables of Crystallography, Vol. 4*, Table 2.3.1., Kynoch Press, Birmingham, UK, 1974.

29 B.A. Frenz: *The Enraf-Nonius CAD4 SDP System, Computing in Crystallography*, Delft University Press, Delft, Holland, 1978, p. 64.

30 W. Scherer, P. Kiprof, E. Herdtweck, R.E. Schmidt, M. Birkhahn and W. Massa, *STRUX-IV, ein Programm zur Verarbeitung von Röntgendaten,* Universität Marburg (1985) und Technische Universität München (1990), Germany.

31 C.K. Johnson, *ORTEP, a Fortran Thermal Ellipsoid Plot Program for Crystal Structure Illustrations*, Oak Ridge National Laboratory, Tennessee, USA, 1965.